Can a penalized-likelihood estimation algorithm be used to reduce the injected dose or the acquisition time in 68Ga-DOTATATE PET/CT studies?

Alexandre Chicheportiche (alexandre@hadassah.org.il)
Hadassah Medical Center https://orcid.org/0000-0001-7804-7421
Elinor Goshen
Edith Wolfson Medical Center
Jeremy Godefroy
Hadassah Medical Center
Simona Grozinsky-Glasberg
Hadassah Medical Center
Kira Oleinikov
Hadassah Medical Center
Amichay Meirovitz
Hadassah Medical Center
David J. Gross
Hadassah Medical Center
Simona Ben-Haim
Hadassah Medical Center

Original research

Keywords: Q.Clear reconstruction, reduced acquisition time/injected dose, image quality, visual evaluation, 68Ga-DOTATATE

Posted Date: June 11th, 2020

DOI: https://doi.org/10.21203/rs.3.rs-34588/v1

Version of Record: A version of this preprint was published on February 12th, 2021. See the published version at https://doi.org/10.1186/s40658-021-00359-6.

Abstract

Background: Both image quality and quantitative accuracy of PET depend on several factors such as uptake time, scanner characteristics and image reconstruction methods. Ordered subset expectation maximization (OSEM) is considered today the gold standard for image reconstruction. Penalized-likelihood estimation (PL) algorithms have been recently developed for PET reconstruction to improve quantitation accuracy while maintaining or even improving image quality. In the present study, we aim to compare the performance of a PL algorithm (Q.Clear, GE Healthcare) and 3D OSEM for 68Ga-DOTATATE (68Ga-DOTA) PET studies, both visually and quantitatively. Thirty consecutive whole-body 68Ga-DOTA studies were included. The data were acquired in list mode and reconstructed using 3D OSEM and Q.Clear with various values of the regularization parameter β, and various acquisition times per bed position (bp), thus generating images with reduced injected dose (1.5 min/bp: β=300-1100; 1.0 min/bp: β=600-1300 and 0.5 min/bp: β=800-2200). Evaluation was performed using a phantom and clinical data. Finally, two experienced nuclear medicine physicians blinded to the variables assessed the image quality visually.

Results: Clinical images reconstructed with Q.Clear , set at 1.5 and 1.0 min/bp using β = 1100 and 1300 respectively, resulted in images with noise equivalence to 3D OSEM (1.5 min/bp) with a mean increase in SUVmax of 14 % and 11%, in SNR of 18% and 10%, and in SBR of 14% and 12%, respectively. Reconstruction using 0.5 min/bp and β = 2200 resulted in SUVmax, SNR and SBR with a relative difference < 1%. Visual assessment yielded similar results with mean scores for Q.Clear (1.5, 1.0 and 0.5 min/bp) vs 3D OSEM (1.5 min/bp) of 3.58 vs 3.38, 3.64 vs 3.47 and 3.60 vs 3.61, respectively.

Conclusion: 68Ga-DOTA reconstructions with Q.Clear, 1.5 and 1.0 min/bp resulted in increased tumor SUVmax and in improved SNR and SBR at a similar level of noise compared to 3D OSEM. Q.Clear with β =1300 enabled a one-third reduction of acquisition time or injected dose, with similar image quality compared to 3D OSEM.

Background

Positron emission tomography (PET) computed tomography (CT) with ^{68}Ga-DOTATATE (^{68}Ga-DOTA) is widely used for imaging of neuroendocrine tumors. with significant roles in staging, assessment of somatostatin receptor status, and decision-making regarding therapy regimens. The current procedure guidelines for PET/CT tumor imaging with ^{68}Ga-DOTA-conjugated peptides [1] recommends an injected activity ranging between 100 and 200 MBq depending essentially on the characteristics of the PET tomograph. In order to reduce patient dose, and considering that ^{68}Ga-DOTA availability is limited by ^{68}Ge/^{68}Ga generator capacity, reduced injected doses with preserved image quality should be investigated, with the ultimate aim of defining the most appropriately low level of injected activities.

Image quality and quantitative accuracy of PET studies are highly influenced by several factors such as injected activity, uptake time, scanner characteristics and image reconstruction methods. Currently,

statistical iterative reconstruction methods are the most widely used image reconstruction methods [2] and the ordered subset expectation maximization (OSEM) statistical method is the gold standard. OSEM algorithms approach the acquired image by successive updated approximations, repeated until the difference between the projections of the reconstructed image and the actually recorded one falls below a specific level. The major drawback of OSEM is that the iteration process has to be stopped before convergence in order to avoid image degradation due to excessive noise increase [3]. This leads to a bias in the final image estimate toward the initial image and to a decrease in contrast recovery (CR), signal-to-noise ratio (SNR) and image quality, which is partly be accountable to the ineffective convergence of the algorithm.

Penalized-likelihood estimation (PL) reconstruction algorithms have been recently developed and clinically implemented to improve quantitation accuracy, while maintaining or even improving image quality. PL algorithms allow for fully convergent iterative reconstruction, leading to higher image contrast than for OSEM while limiting noise [4]. For PL algorithms, a single positive regularization parameter controls the trade-off between noise level and resolution, as opposed to several iterations, subsets and post-filter with OSEM.

Q.Clear is the commercially available version of the PL algorithm introduced by GE Healthcare. The only user-input variable it utilizes, ie. the positive penalization parameter, is named the β factor. Q.Clear has been shown to provide better quantitation accuracy and image quality than OSEM in both phantom and clinical ^{18}F-FDG studies [5–8]. An optimal penalization parameter of 400 has been defined for ^{18}F-FDG examinations [5, 7]. A recent study [9], showed that using a β factor between 300 and 450, Q.Clear is superior to OSEM including Time-of-Flight (TOF) information and point spread function modeling, in terms of CR and SNR. For ^{68}Ga-DOTA, the optimal regularization parameters are not yet well defined. One preliminary study by Lantos *et al.* [10] in 10 patients suggested using a β factor between 350 and 450 in clinical practice, for all the studied radiopharmaceuticals while the study conducted by ter Voert et *al*. [11] concluded that, for ^{68}Ga-PSMA a β value between 400 and 550 could be optimal. However, based on preliminary visual observations, higher penalization factor values seemed to us more adequate.

In the present study we aimed to evaluate the performance of Q.Clear with full and reduced acquisition time/injected activity, compared to OSEM + TOF + PSF with no time/dose reduction for whole body ^{68}Ga-DOTA examinations. We defined an optimal β value for the standard acquisition time and we investigated optimal β values leading to similar or even superior image quality while the acquisition time / injected activity had been reduced. To achieve this goal Q.Clear and OSEM acquisitions were compared by quantitative evaluation of phantom acquisitions and clinical studies, as well as by qualitative assessments.

Methods

Patient Population

Between March 17, 2019, and June 19, 2019, 65 consecutive patients underwent ^{68}Ga-DOTA PET/CT scans at our institution. Inclusion criteria for this study were (a) images were acquired on General Electric (GE) Healthcare Discovery MI PET/CT scanner (Milwaukee WI, USA) and (b) at least one focus of pathological ^{68}Ga-DOTA uptake was noted on the PET/CT study.

Of the 65 patients 25 patients were excluded, including 21 patients with normal studies and 14 patients who underwent ^{68}Ga-DOTA PET/CT on another PET/CT system (Discovery MI-DR, GE Healthcare) at our institution. The remaining 30 patients (19 men, 11 women; mean ± SD, 58 ± 19 years old; range 11–83 years) were included in this single-center retrospective study.

Data Acquisition

All studies were performed on a Discovery MI PET/CT (GE Healthcare). The system combines a 128-slice computed tomography (CT) system and a 4-ring PET system with LightBurst digital detectors providing a 20-cm axial field-of-view and a 70-cm transaxial field-of-view. The system is TOF-capable with a timing resolution of 377 ps [12].

Phantom Acquisition. The National Electrical Manufacturers Association (NEMA) IEC image quality body phantom (IQBP) (Model PET/IEC-BODY/P) [13] was used to provide an overall assessment of the imaging capabilities of the system in different conditions. The phantom contains spheres with an internal diameter of 10, 13, 17, 22, 28, and 37 mm and a 50-mm diameter cylindrical insert mounted in the center. All the spheres were filled with radioactive material (^{68}Ga) and lung insert provided with the phantom was filled with low-density material (polystyrene) and water. The phantom background region and spheres contained a ^{68}Ga activity concentration of 2.48 kBq/mL and 9.92 kBq/mL, respectively, at the time of the acquisition.

Clinical Images. ^{68}Ga-DOTA was injected intravenously. The mean administered activity was 166.1 ± 38.3 MBq (range,103.6–262.7 MBq). The PET acquisition started at a mean of 68 ± 10 min (range, 53–91 min) after tracer injection. All PET studies were performed from the proximal femur to the base of the skull and were acquired in list-mode with an acquisition time of 1.5 min per bed position (bp).

Patients' characteristics, injected dose and uptake time are summarized in Table 1.

Table 1
Demographic data and patient characteristics

Pt #	Age (yo)	Body weight (kg)	Dose (MBq)	Uptake time (min)	Primary tumor	Primary tumor site	Sites of metastases
1	78	59	170.2	74	Small bowel NET	Resected	Liver, LN above and below the diaphragm
2	73	100	155.4	69	Pheochromocytoma	Local recurrence in right adrenal bed	Retroperitoneal LN, omentum
3	68	97	199.8	58	Lung NET	Resected	Mediastinal LN, bones
4	46	71	188.7	61	Pancreatic NET	Pancreas	Mesenteric, retroperitoneal LN, liver, bones
5	28	70	144.3	76	Pancreatic NET	Pancreas	(nonconclusive bone focus, resolved on FUP)
6	11	43	155.4	62	Lung carcinoid	Lung mass	Mediastinal LN
7	64	53	133.2	76	Pancreatic NET	Local recurrence in surgical bed	Liver, Liver hilum LN, bones
8	66	68	159.1	70	Lung NET	Lung several foci	Mediastinal and right hilar LN
9	60	59	159.1	54	Glucagonoma	Local recurrence in surgical bed	Mesenteric LN, mediatinal LN, bones
10	83	65	159.1	81	Pancreatic NET	Pancreas	Right iliac crest and mediastinal LN
11	79	60	159.1	57	Unknown origin	Unknown	Liver, bone
12	27	53	173.9	62	Bronchial carcinoid	Resected	Bones, soft tissue
13	49	65	122.1	65	Pancreatic NET	Pancreas	Liver
14	66	59	136.9	74	Pancreatic NET	Resected, local recurrence	Liver

Pt #	Age (yo)	Body weight (kg)	Dose (MBq)	Uptake time (min)	Primary tumor	Primary tumor site	Sites of metastases
15	67	75	162.8	74	Small bowel NET	Resected	Pancreas, liver
16	70	119	203.5	63	Appendiceal carcinoid	Resected	Liver
17	71	59	148	78	Pancreatic NET	Pancreas	Liver
18	73	110	247.9	79	Pancreatic NET	Pancreas	N/A
19	13	40	129.5	53	Insulinoma	Pancreas	Liver, retroperitoneal LN
20	38	83	111	88	Pancreatic NET	Pancreas	LN above and below the diaphragm
21	75	72	122.1	91	Lung NET	Lung	Brain
22	72	88	140.6	58	Small bowel NET	Resected	Liver, omentum
23	59	46	166.5	61	Small bowel NET	Resected	Liver hilum LN
24	56	71	103.6	73	Pancreatic NET	Resected	Liver, bones
25	38	65	262.7	72	Lung NET	Lung	N/A
26	60	63	185	57	Small bowel NET	Resected	Liver
27	65	80	144.3	78	Medullary Thyroid Ca	Left lobe resected	Surgical bed
28	42	72	222	59	Small bowel NET	Resected	Liver, mesenteric LN
29	74	66	185	69	Paraganglioma	Resected	Local recurrence (brain), bone
30	70	84	233.1	58	Unknown origin	Unknown	Bones, right hilum
mean ± SD	58 ± 19	71 ± 18	166.1 ± 38.3	68 ± 10	-	-	-

NET = Neuroendocrine Tumor ; LN = Lymph Node ; FUP = Follow-up Plan

Image Reconstruction

Phantom and clinical images were first reconstructed with 1.5 min/bp and using the GE VUE Point FX-S algorithm (VPFX-S), a 3D maximum likelihood ordered subset expectation maximization (3D OSEM)

image reconstruction algorithm using TOF information and point spread function modeling (3 iterations, 8 subsets, 6 mm postprocessing filter). These seetings were recommended by the manufacturer for ^{68}Ga-DOTA studies and the corresponding reconstructed images were considered as gold standard.

In addition, data were reconstructed using the Q.Clear algorithm with different values of the penalization factor β and with 1.5 min/bp, 1.0 min/bp and 0.5 min/bp acquisitions. The 1.5, 1.0 and 0.5 min acquisitions were used to simulate standard, two thirds and one third acquisitions (time or injected dose). Images were reconstructed with β = 300, 400, 500, 600, 700, 800, 1000 and 1100 for the 1.5 min/bp acquisition, β = 600, 700, 800, 1000, 1100, 1200, and 1300 for the 1.0 min/bp acquisition and β = 800, 1000, 1200, 1300, 1400, 1500, 1600, 1800, 2000 and 2200 for the 0.5 min/bp acquisition. These values were chosen following an initial subjective visual assessment of clinical images performed by one of the authors (AC, who was not involved in the blinded visual assessment of the studies).

All data were corrected for scatter, random events, dead time, and attenuation (using CT).

Image Analysis

Images were analysed as previously described by Lindström *et al.* [14].

Phantom Data. Background variability (BV) and contrast-to-noise ratio (CNR) were calculated and compared. BV was defined as the SD of the activity concentration in large ROIs located away from the axial plane containing the sphere centers, divided by the mean activity concentration in these background ROIs. CNR was calculated as contrast recovery (CR) divided by BV as follows:

$$CNR = CR/BV \qquad \text{Eq. 1}$$

$$\text{where } CR = (C_H / C_B - 1) / (a_H / a_B - 1)$$

with C_H and C_B, counts and a_H and a_B, activities in hot spheres and background ROIs, respectively. Image analysis was done on a GE Healthcare Advantage Workstation (AW 3.2 Ext. 3.2, 2019).

Clinical Images. Level of noise, signal-to-noise ratio (SNR) and signal-to-background ratio (SBR) were calculated and compared. Level of noise was defined as SUV_{std} of a large spherical VOI in normal liver normalized to SUV_{mean} of the same VOI. SNR was calculated as lesion SUV_{max} divided by noise level. SBR was defined as lesion SUV_{max} divided by SUV_{mean} of the normal liver VOI. For this analysis up to three lesions per study were delineated on the AW Workstation using a 41% SUV_{max} threshold. Lesions VOIs were first built on VPFX-S (3D OSEM + TOF + PSF) images and bookmarks containing the location of these lesions were used to propagate and build new VOIs on reconstructed images with 41% thresholding. Finally, lesions SUV_{max} values obtained for VPFX-S and the reconstructed algorithm leading to similar level of noise were also analyzed and compared.

Blinded Visual Assessment. In the standard acquisition and in each of the simulated reduced injected activity studies, the five Q.Clear reconstructions leading to the best results in phantom and clinical

images evaluations were visually compared with the gold standard VPFX-S reconstruction by two blinded experienced nuclear medicine physicians (EG and SBH). A total of 90 image sets were assessed; every set consisted of 5 different reconstructions for 1.5, 1.0 and 0.5 min/bp, for each of the 30 patients included in the study. All data were anonymized regarding the reconstruction method and numbers were randomly assigned. PET datasets were rated on a 4-point scale (1 = very poor/nondiagnostic; 2 = poor; 3 = good and 4 = very good) for contrast, sharpness, noise, liver homogeneity, tumor detectability and overall image quality.

Statistical Analysis

The mean values for each of the rated parameters by the two readers and the mean values of all scores were summarized. A paired Student *t* test was used to evaluate differences in rating between the different image reconstruction methods. Statistical significance was defined as $p < 0.05$.

Results

Phantom Studies

Background variability and contrast-to-noise ratio obtained from images reconstructed with the gold standard method (VPFX-S, 1.5 min/bp) and Q.Clear with different values of the penalization factor β and acquisition times of 1.5 min/bp, 1.0 min/bp and 0.5 min/bp are shown in Fig. 1a-c. The Q.Clear algorithm with $\beta \geq 1000$ for 1.5 min/bp, $\beta \geq 1200$ for 1.0 min/bp and $\beta \geq 2000$ for 0.5 min/bp allowed for similar or improved BV values compared to the gold standard reconstruction method. Similarly, CNR values obtained with Q.Clear are higher than VPFX-S when using $\beta \geq 1000$ for 1.5 min/bp and $\beta = 1300$ for 1.0 min/bp. For 0.5 min/bp, improved CNR results are reached for $\beta = 2000$, 2200 for the large 28 and 37 mm spheres while for the 17 and 13 mm spheres CNR values were about 25% and 35% lower compared to the gold standard. Of note, in all reconstructions, the standard reconstruction led to better CNR for the smallest 10 mm diameter sphere.

Figure 2 presents the transverse views of the phantom acquisitions, reconstructed with the VPFX-S algorithm with 1.5 min/bp and with Q.Clear for different values of β and different acquisition times per bed position (1.5, 1.0 and 0.5 min/bp). The images demonstrate better BV with increasing β factor for all the acquisition times.

Clinical Images

Figure 3a-c presents the SNR, SBR and noise level values calculated from the 30 clinical studies reconstructed using Q.Clear with 1.5, 1.0 and 0.5 min/bp respectively, and normalized to gold standard SNR, SBR and noise level values. A total of 75 lesions per reconstruction were used for comparative analysis of the SNR and SBR obtained using Q.Clear, with different β values and acquisition times, to those obtained with the VPFX-S reconstruction and 1.5 min/bp. As described above, a single large normal

liver VOI was used in each study for noise level comparison, for a total of 30 measurements per reconstruction.

Regardless of the acquisition time per bed position the choice of the penalization factor influenced the different parameters, resulting in improvement of the noise level and the SNR and degradation of SBR for increasing β values. For the smallest β values used in this study (i.e. β = 300 for 1.5 min/bp, β = 600 for 1.0 min/bp and β = 800 for 0.5 min/bp) the noise level increased by about 85%, 50% and 65% on average, respectively, compared to the gold standard reconstruction method. The difference dropped to less than 1% for the highest β values (i.e. β = 1100 for 1.5 min/bp, β = 1300 for 1.0 min/bp and β = 2200 for 0.5 min/bp). For the latter, the SNR increased by 19% and 10% for 1.5 min/bp and 1.0 min/bp on average, respectively. Similarly, the SBR was also higher than the gold standard with a mean increase of 14% and 12% and the SUV_{max} increased by 14% and 11% on average, respectively. For 0.5 min/bp, the mean SNR and SBR values were similar to those obtained with the VPFX-S algorithm. The SUV_{max} decreased by about 1%. Furthermore, β values of 1000 for 1.5 min/bp and 1200 for 1.0 min/bp, respectively, had similar noise levels with < 5% difference and with improved SNR of 17% and 8% and improved SBR of 18% and 16%, respectively.

Visual Assessment

Five Q.Clear reconstructions (i.e. β = 600–1100 for 1.5 min/bp, β = 800–1300 for 1.5 min/bp, β = 1500–2200 for 1.5 min/bp) were compared with the gold standard reconstruction. Figure 4a-c shows the mean grades given by the two readers for the following image quality parameters: overall image quality, contrast, sharpness, noise level, liver homogeneity and tumor detectability, for VPFX-S, 1.5 min/bp and Q.Clear reconstructions with 1.5, 1.0 and 0.5 min/bp, respectively. Also shown are the mean values of all aspect scores.

For the full time acquisition (1.5 min/bp) Q.Clear reconstruction with β = 1100 yielded the highest mean grade of all parameters with a score of 3.59 and $p < 10^{-6}$ (Fig. 5). Reconstructions with β = 800 and 1000 also ranked better than VPFX-S with mean scores of 3.57 ($p < 2 \bullet 10^{-6}$) and 3.49 ($p < 0.01$), respectively, compared to 3.38 for the gold standard. Similarly, 1.0 min/bp images reconstructed with Q.Clear and β = 1100, 1200 and 1300 scored better than VPFX-S with 1.5 min/bp with $p < 0.02$, $3 \bullet 10^{-5}$ and $3 \bullet 10^{-7}$, respectively. However, for 0.5 min/bp Q.Clear scored 3.60 for β = 2200 compared to 3.61 for VPFX-S with 1.5 min/bp ($p = 0.39$). Of note, for all β values assessed here, regardless of acquisition time, the Q.Clear algorithm presented a definite advantage in terms of contrast and sharpness compared to VPFX-S with p values < 0.01 in all cases (Fig. 6). Q.Clear also provided improved tumor detectability with a maximum score of for 3.97 vs 3.91 for VPFX-S for 1.5 min /bp and and 4.0 vs 3.98 for VPFX-S for 1.0 min/bp. For 0.5 min/bp Q.Clear degraded tumor detactability with a maximum score of 3.87 vs 3.97 for VPFX-S (Fig. 7).

Discussion

The present study focused on determining optimal β values for ^{68}Ga-DOTA studies for standard settings and for when the acquisition time/injected activity is reduced by one and two thirds. Phantom evaluation allowed us to determine that using the Q.Clear algorithm with $\beta \geq 1000$ for 1.5 min/bp and $\beta \geq 1200$ for 1.0 min/bp similar or improved BV and CNR values are obtained. However, the results showed that for 0.5 min/bp, improved CNR results are reached for $\beta = 2000$, 2200 for the large spheres but reduced by about 30% for the small volumes. This last observation can be related to the visualization assessment results obtained for 0.5 min/bp where the tumor detectability was degraded in comparison to 3D OSEM. For 1.5 and 1.0 min/bp, Q.Clear improved tumor detectability for all lesions although phantom evaluation results suggested a detectability degradation for 10 mm lesions. Evaluation of noise, SNR and SBR on clinical studies suggested that optimal β values would be of 1000, 1100 for 1.5 min/bp and 1200, 1300 for 1.0 min/bp and of 2200 for 0.5 min/bp. Finally, in view of visualization assessment results, the optimal β factors were 1100 for 1.5 min/bp and 1300 for 1.0 min/bp. For 0.5 min/bp acquisitions, Q.Clear did not demonstrate a clear advantage compared to VPFX-S with 1.5 min/bp. Indeed, the maximum β value evaluated in the present study for 0.5 min/bp was 2200, and this was not sufficiently high to obtain statistically significant improvement of results compared to the gold standard reconstruction. For 1.5 and 1.0 min/bp the *p* value of the differences between the gold standard and Q.Clear decreases quickly from a given β value (Fig. 5). For 0.5 min/bp, the maximum value of β considered here did not allow to reach this drop point. In view of the image quality improvement with increasing β for 1.5 and 1.0 min/bp, it would be interesting to investigate higher β values, increasing to the point of decreasing image quality, in order to determine if there is a more optimal β for these acquisition times.

The two physicians who assessed the images first read a training case in consensus in order to determine the scoring method. For overall image quality, the physicians chose to focus essentially on noise in the images. As a matter of fact, overall image quality and noise level obtained similar scores, regardless of the acquisition time (Fig. 4). This may induce a bias in the scoring, leading to a decrease in final Q.Clear score. Moreover, when rating a new technique versus a well-known one, observers are more familiar with the latter and consider it as gold standard. Physicians might therefore have been biased and rated OSEM outcomes higher than Q.Clear results.

Clinical images were evaluated to assess the improvement in SNR and SBR using Q.Clear with different β values and acquisition times compared to the gold standard VPFX-S, 1.5 min/bp. The box plots showed mostly a positive skew distribution indicating frequent SNR or SBR values in the lower part of the box and few high values with some outliers (Fig. 3). The outliers had up to 2.5 times SNR and 4 times SBR improvement using Q.Clear compared to VPFX-S. To evaluate the origin of these outliers, an analysis of the SNR and SBR as a function of the lesion size, injected activity, patient weight and value of the penalization factor has been performed. The improvement in SNR and SBR respectively using Q.Clear, 1.5 min/bp as a function of the lesion size and the β value for the 75 tumors included in the study (Fig. 8a-b) shows that small lesions with volumes lower than 1–2 cm^3 had the highest improvement in both SNR and SBR, corresponding to the outliers observed in Fig. 3. This is in accordance with previous observation by Lindström *et al.* [14] where the relative difference in SUV_{max} between Q.Clear and 3D

OSEM was larger for smaller lesions. For larger lesions, the improvement for a given β remained stable as a function of the lesion volume. Moreover, for small lesions an increase of β lead to a decrease in the SNR improvement while for larger lesions an increase of β lead to improved SNR (Fig. 3). Analysis of the SNR and SBR as a function of the injected dose per kilogram or uptake time did not show any clear dependence, with the SNR or SBR improvement staying stable despite variation of these parameters.

There are several limitations to our study. First, only 30 patients were included in this work. This limitation is due to the time consuming task of the reconstruction. Indeed, each study has been reconstructed for different values of β and acquisition times for a total of 25 reconstructions per study or 750 reconstructions for the 30 included studies, each reconstruction taking approximately 3–5 minutes. Assessment in a larger patient cohort would allow a more certain implementation in clinical practice. Moreover, this limitation prevented us from reconstructing studies with additional β values using Q.Clear than those defined initially. Finally, our study has been conducted on a specific PET/CT system, the Discovery MI. It would be interesting to investigate and confirm the β values found here on other systems of the same and different vendors with different PL algorithms.

Conclusion

^{68}Ga-DOTA studies reconstrtucted with Q.Clear, the penalized-likelihood estimation reconstruction algorithm developed by GE, and adequate values of the penalization factor β resulted in increased tumor SUV_{max} and in improved SNR and SBR at a similar level of noise compared to 3D OSEM for 1.5 and 1.0 min/bp. The optimal β value for 1.5 min/bp was 1100, lead to better image quality than the gold standard VPFX-S (3D OSEM + TOF + PSF). Q.Clear allowed for a one third shorter acquisition resulting in better image quality than VPFX-S with 1.5 min/bp when using β = 1300. However, for 0.5 min/bp the β values considered here did not allow to obtain significantly improved results compared to the gold standard. Therefore, one third lower injected activities or acquisitions could be considered for ^{68}Ga-DOTA studies using the Q.Clear algorithm.

Abbreviations

OSEM
Ordered subset expectation maximization
PL
Penalized-likelihood estimation
bp
Bed position
PET
Positron emission tomography
CT
Computed tomography
TOF

Time-of-Flight

GE

General Electric

NEMA

National Electrical Manufacturers Association

IQBP

Image quality body phantom

VPFX-S

VUE Point FX-S algorithm

CR

Contrast recovery

SNR

Signal-to-noise ratio

BV

Background variability

CNR

Contrast-to-noise ratio

SBR

Signal-to-background ratio

Declarations

Ethics approval and consent to participate

All procedures performed in studies involving human participants were in accordance with the ethical standards of the institutional and/or national research committee and with the 1964 Helsinki declaration and its later amendments or comparable ethical standards. For this type of study, formal consent is not required.

Consent for publication

Not applicable.

Availability of data and materials

Patient imaging was done in the scope of the routine clinical diagnostic studies, and the raw data are stored in the hospital archiving system at the Hadassah-Hebrew University Medical Center, Jerusalem, Israel.

Competing interests

The authors declare that they have no conflict of interest.

Funding

Not applicable.

Authors’ contributions

Dr. AC contributed to the design of this work.

Dr. JG and Prof. SBH were in charge of imaging studies and interpretation of images.

Dr. AC performed the quantitative analysis.

Dr. EG and Prof. SBH performed the image quality assessment.

Drs. AC, EG and Prof. SBH wrote the manuscript.

Drs. SG-G, KO, AM , JG and Prof. DJG revised the manuscript.

All authors read and approved the final manuscript.

Acknowledgments

The authors would like to thank Moshe Sasson for helpful discussions and suggestions.

Authors' information

Dr. AC, Phd (ORCID iD: 0000-0001-7804-7421) ; Dr. EG, MD; Dr. J G, MD, MsC; Dr. SG-G, MD ; DR. KO, MD ; Dr. AM, MD ; Prof. DJG, MD ; Prof. SBH, MD, DSc;

[1] Department of Nuclear Medicine & Biophysics, Hadassah-Hebrew University Medical Center, 91120 Jerusalem, Israel. [2] Department of Nuclear Medicine, Wolfson Medical Center, 58100 Holon, Israel

[3] Neuroendocrine Tumor Unit, ENETS Center of Excellence, Endocrinology and Metabolism Department, Hadassah-Hebrew University Medical Center, 91120, Jerusalem, Israel [4] Oncology Department and Radiation Therapy Unit, Hadassah-Hebrew University Medical Center, 91120, Jerusalem, Israel [5] Faculty of Medicine, Hebrew University of Jerusalem, 91120, Jerusalem, Israel [6] Institute of Nuclear Medicine, University College London and UCL Hospitals NHS Trust, London, United Kingdom.

References

1. Virgolini I, Ambrosini V, Bomanji JB, Baum RP, Fanti S, Gabriel M, et al. Procedure guidelines for PET/CT tumour imaging with 68 Ga-DOTA-conjugated peptides: 68 Ga-DOTA-TOC, 68 Ga-DOTA-NOC, 68 Ga-DOTA-TATE. Eur J Nucl Med Mol Imaging. 2010;37:2004–10.
2. Hudson HM, Larkin RS. Accelerated image reconstruction using ordered subsets of projection data. IEEE Trans Med Imaging. 1994;13:601–9.
3. Tong S, Alessio AM, Kinahan PE. Image reconstruction for PET/CT scanners: past achievements and future challenges. Imaging Med. 2010;2:529–45.
4. Zhang J, Maniawski P, Knopp MV. Performance evaluation of the next generation solid-state digital photon counting PET/CT system. EJNMMI Res. 2018;8:97.
5. Teoh EJ, McGowan DR, Macpherson RE, Bradley KM, Gleeson FV. Phantom and Clinical Evaluation of the Bayesian Penalized Likelihood Reconstruction Algorithm Q.Clear on an LYSO PET/CT System. J Nucl Med. 2015;56:1447–52.
6. Ahn S, Ross SG, Asma E, Miao J, Jin X, Cheng L, et al. Quantitative comparison of OSEM and penalized likelihood image reconstruction using relative difference penalties for clinical PET. Phys Med Biol. 2015;60:5733–51.
7. LindstrÃ¶m E, LindsjÃ¶ L, Ilan E, Sundin A, Sorensen J, Danfors T, et al. Optimisation of penalized likelihood estimation reconstruction (Q.Clear) on a digital time-of-flight PET-CT scanner for four different PET tracers. J Nucl Med. 2017;58:1355–5.
8. Sah B-R, Stolzmann P, Delso G, Wollenweber SD, Hüllner M, Hakami YA, et al. Clinical evaluation of a block sequential regularized expectation maximization reconstruction algorithm in 18F-FDG PET/CT studies [Internet]. 2017 [cited 2019 Mar 26]. Available from: https://www.ingentaconnect.com/content/wk/numec/2017/00000038/00000001/art00009.
9. Rogasch JM, Suleiman S, Hofheinz F, Bluemel S, Lukas M, Amthauer H, et al. Reconstructed spatial resolution and contrast recovery with Bayesian penalized likelihood reconstruction (Q.Clear) for FDG-PET compared to time-of-flight (TOF) with point spread function (PSF). EJNMMI Phys. 2020;7:1–14.
10. Lantos J, Mittra ES, Levin CS, Iagaru A. Standard. OSEM vs. regularized PET image reconstruction: qualitative and quantitative comparison using phantom data and various clinical radiopharmaceuticals. Am J Nucl Med Mol Imaging. 2018;8:110–8.
11. Ter Voert EEGW, Muehlematter UJ, Delso G, Pizzuto DA, Müller J, Nagel HW, et al. Quantitative performance and optimal regularization parameter in block sequential regularized expectation maximization reconstructions in clinical 68 Ga-PSMA PET/MR. EJNMMI Res. 2018;8:70.
12. Chicheportiche A, Marciano R, Orevi M. Comparison of NEMA characterizations for Discovery MI and Discovery MI-DR TOF PET/CT systems at different sites and with other commercial PET/CT systems. EJNMMI Phys. 2020;7:4.
13. National Electrical Manufacturers Association. Performance measurements of positron emission tomographs (PET). Rosslyn, USA: NEMA Standards Publication NU 2-2018; 2018.
14. Lindström E, Sundin A, Trampal C, Lindsjö L, Ilan E, Danfors T, et al. Evaluation of Penalized-Likelihood Estimation Reconstruction on a Digital Time-of-Flight PET/CT Scanner for 18F-FDG

Whole-Body Examinations. J Nucl Med. 2018;59:1152–8.

Figures

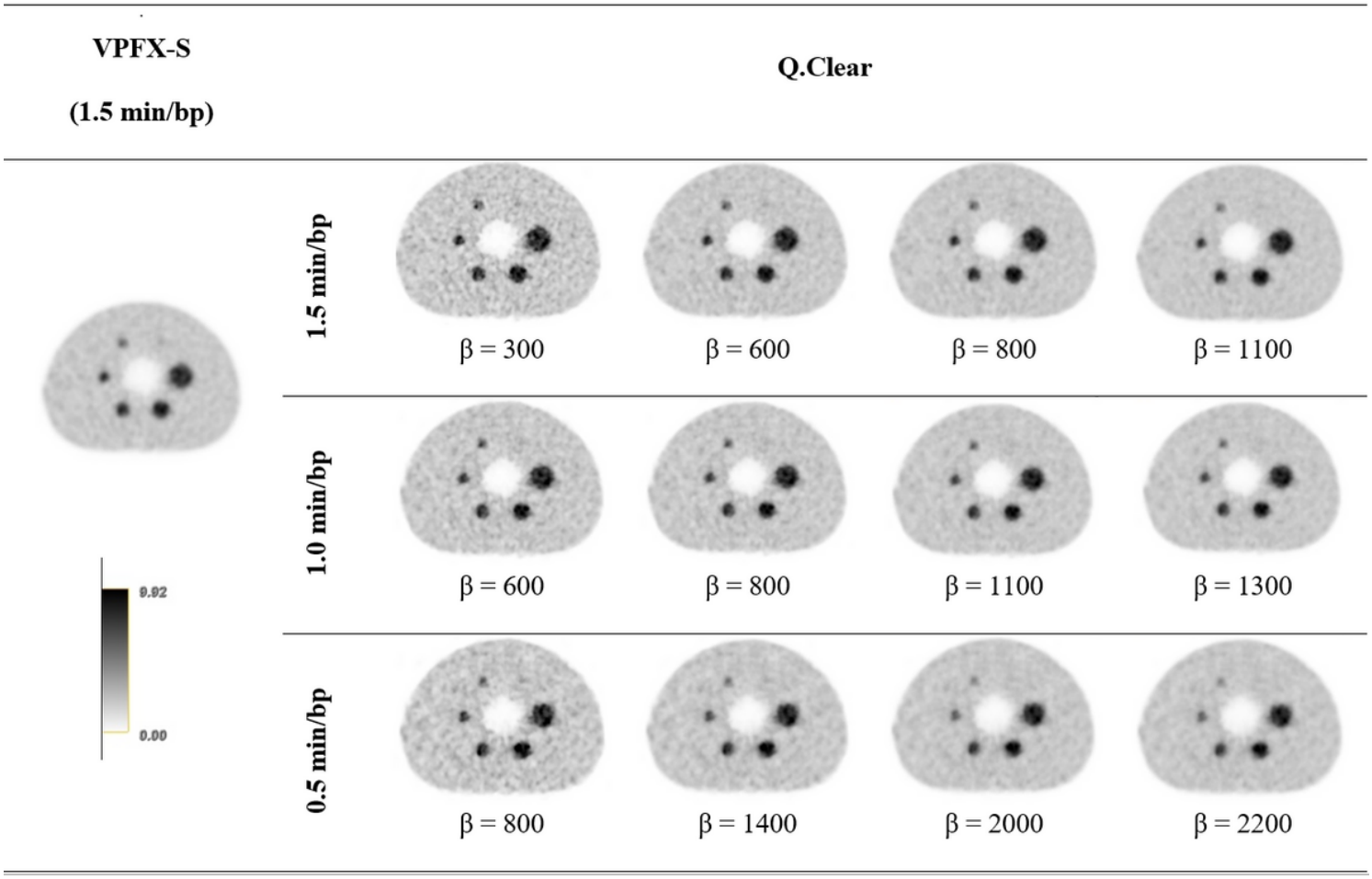

Figure 1

Central slice of the NEMA IEC image quality body phantom reconstructed with the VPFX-S (3D OSEM + TOF + PSF) reconstruction algorithm with 1.5 min/bp and with Q.Clear for different values of β and acquisition time per bed position (1.5, 1.0 and 0.5 min/bp). The gray-scale next represents the activity concentration in kBq/mL for all phatom images.

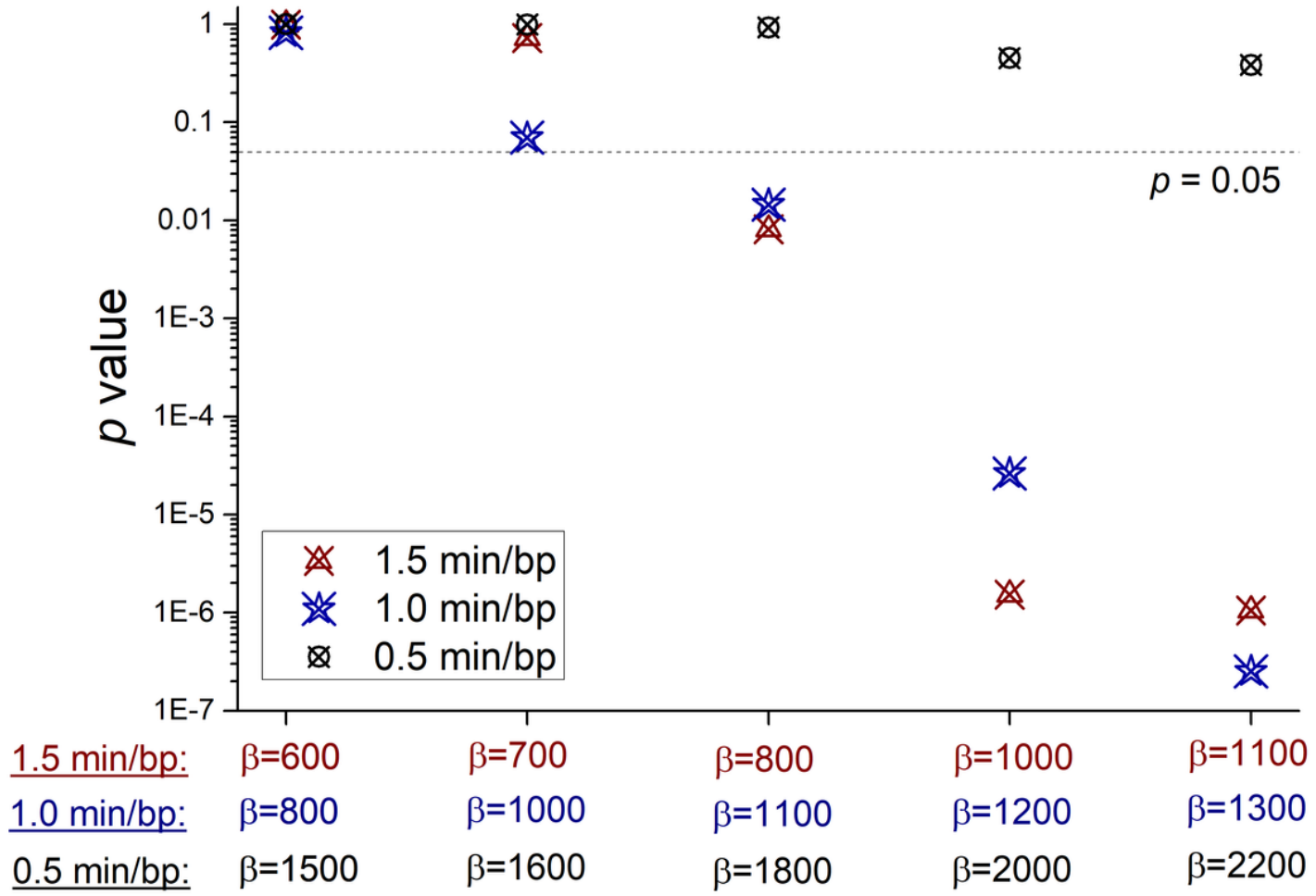

Figure 2

p values (student's t test) of the differences in the mean score of all aspects rated by physicians between reconstructions using Q.Clear with given parameters and the gold standard method (VPFX-S, 1.5 min/bp).

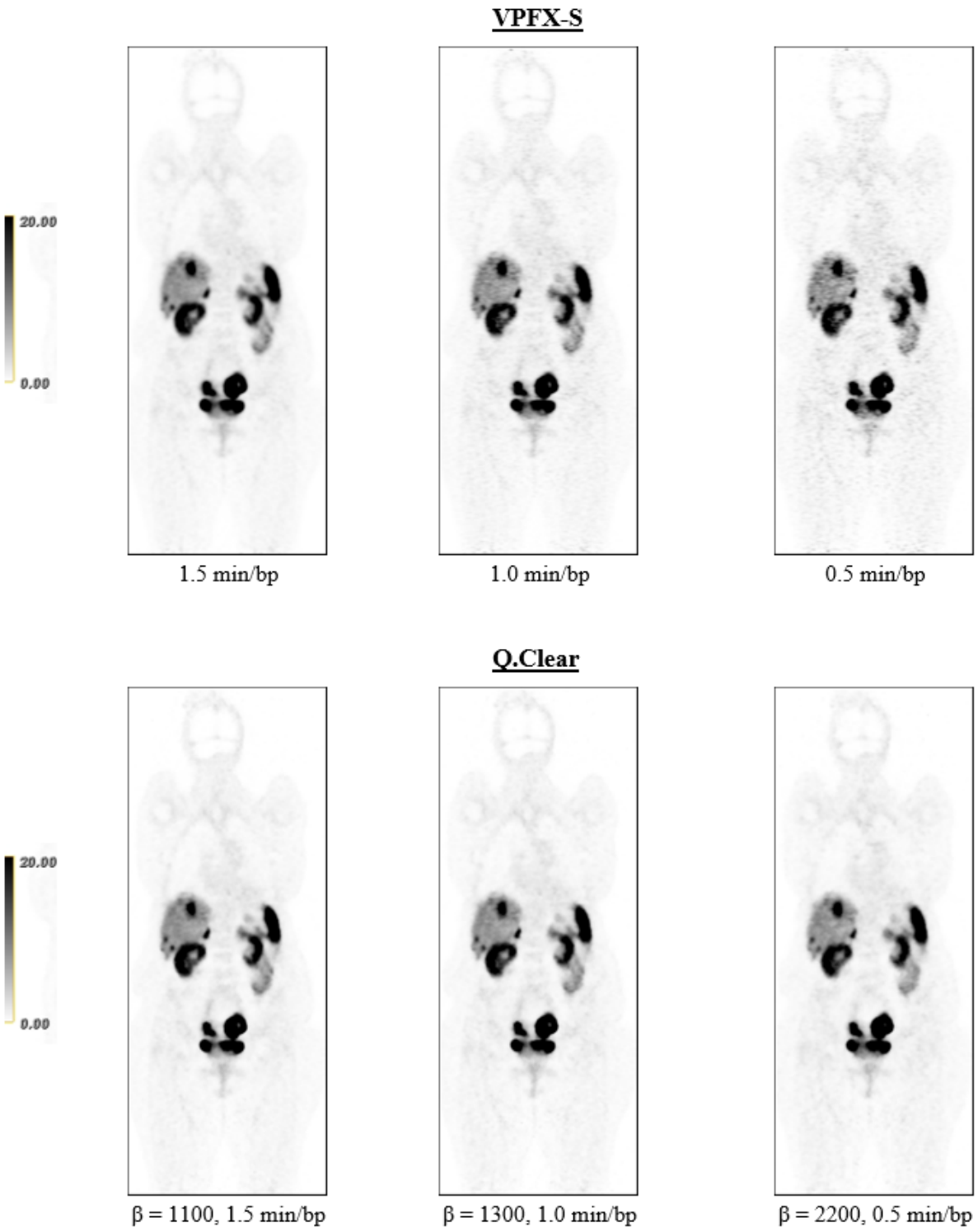

Figure 3

Respresentative coronal 68Ga-DOTA images of patient #1 reconstructed with 3D OSEM TOF PSF (VPFX-S) and Q.Clear, both for 1.5, 1.0 and 0.5 min/bp. The image quality of Q.Clear with 1.0 and 0.5 min/bp is better compared to VPFX-S with the same acquisition time, and is similar to VPFX-S reconstructed with 1.5 min/bp. The gray-scales next to the images represents the corresponding SUV scale in g/ml.

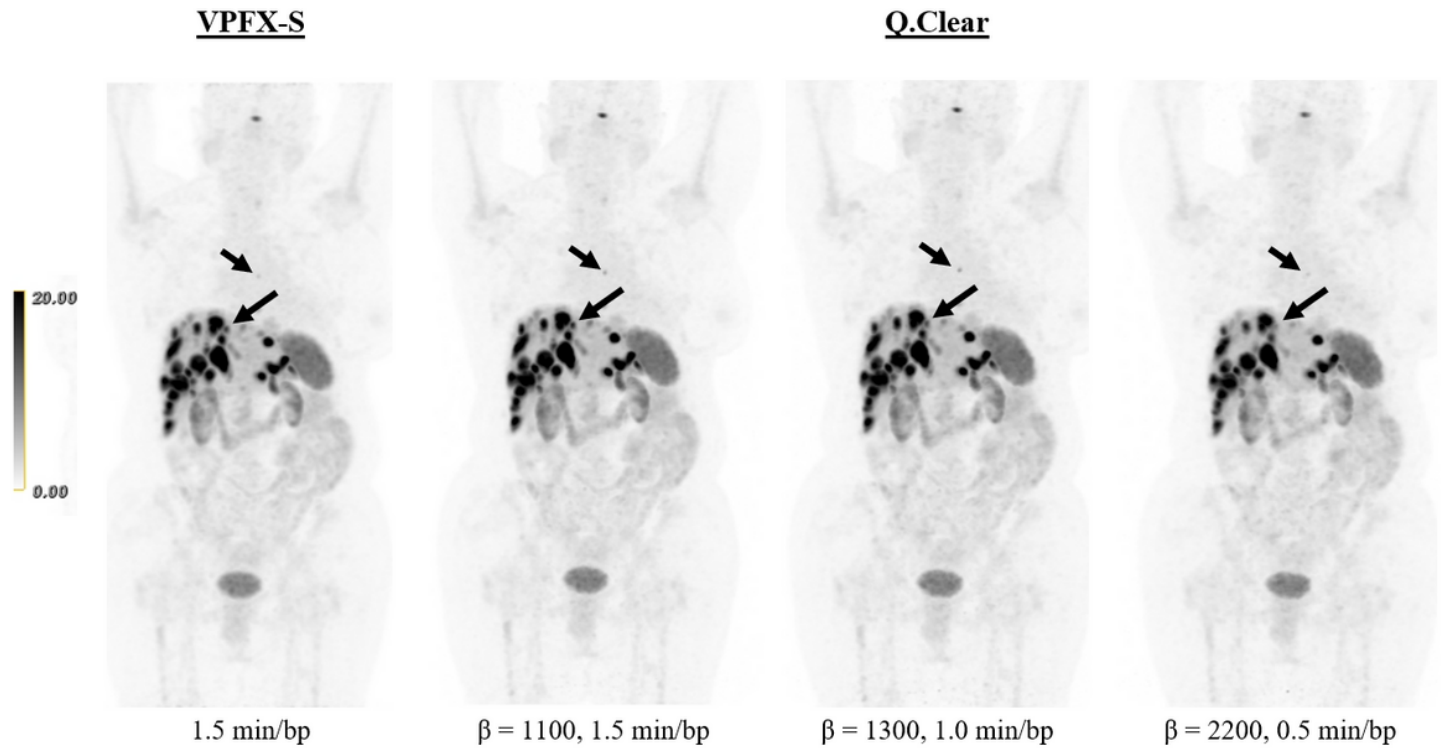

Figure 4

Maximum Intesity Projection (MIP) 68Ga-DOTA images of patient #15 reconstructed with 3D OSEM TOF PSF (VPFX-S), 1.5 min/bp and Q.Clear for 1.5, 1.0 and 0.5 min/bp. Tumor detectability using Q.Clear 1.5 min/bp (β = 1100) and 1.0 min/bp (β = 1300) was better than VPFX-S with 1.5 min/bp, but using Q.Clear 0.5 min/bp (β = 2200) some lesions were missed (arrows). The gray-scale next to the images represents the corresponding SUV scale in g/ml.

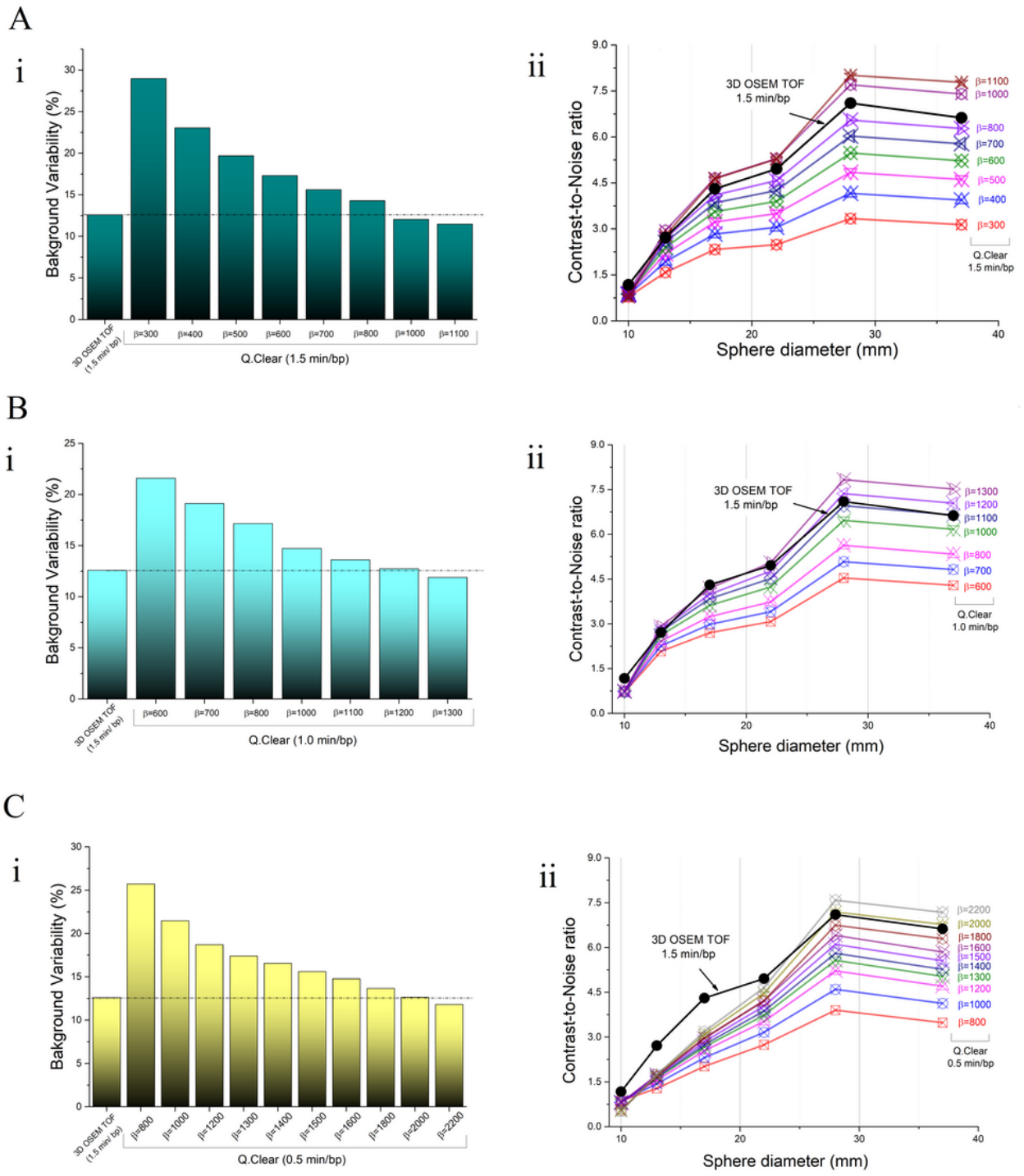

Figure 5

NEMA IEC image quality body phantom (i) background variability and (ii) contrast-to-noise ratio using VPFX-S reconstruction algorithm and, Q.Clear with different values of β and (A) 1.5 min/bp, (B) 1.0 min/bp and (C) 0.5 min/bp.

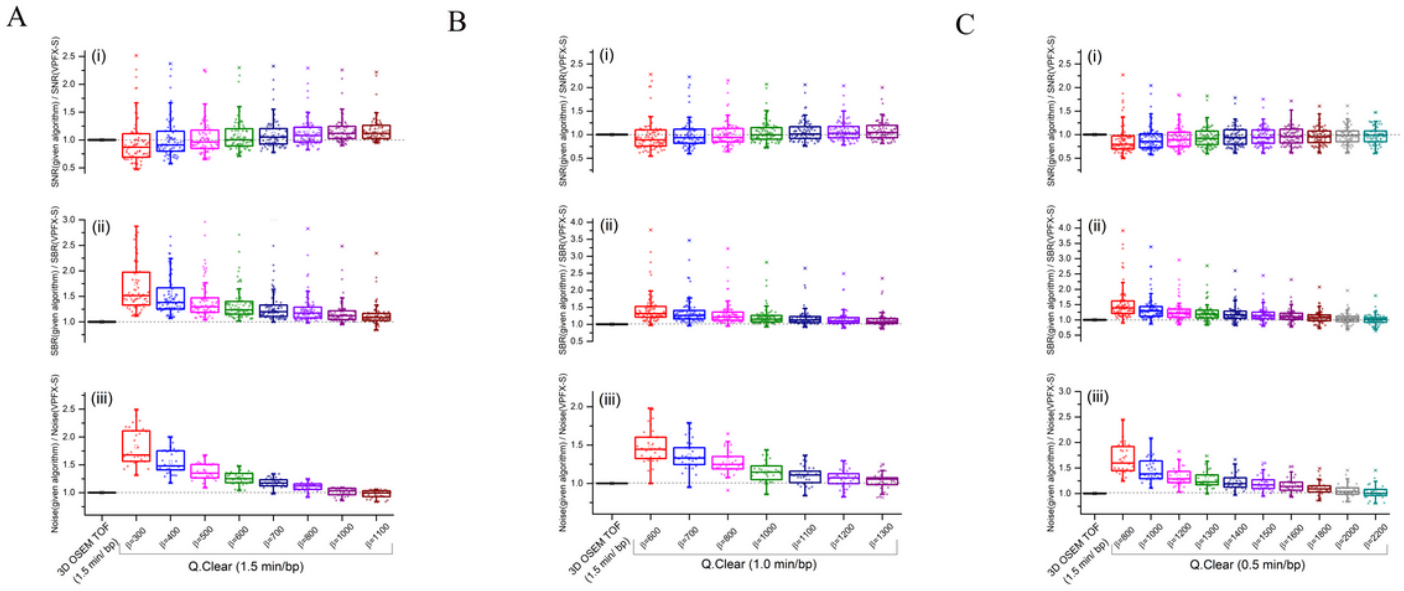

Figure 6

Box plots of (i) SNR, (ii) SBR and (iii) noise level values obtained for 30 clinical studies reconstructed using Q.Clear with various β values and (A) 1.5 min/bp, (B) 1.0 min/bp and (C) 0.5 min/bp and normalized to the values obtained using the gold standard VPFX-S algorithm with 1.5 min/bp. The upper and lower part of the box represent the upper and lower quartile, respectively. The line and the square in the box stand for the median and the mean values, respectively.

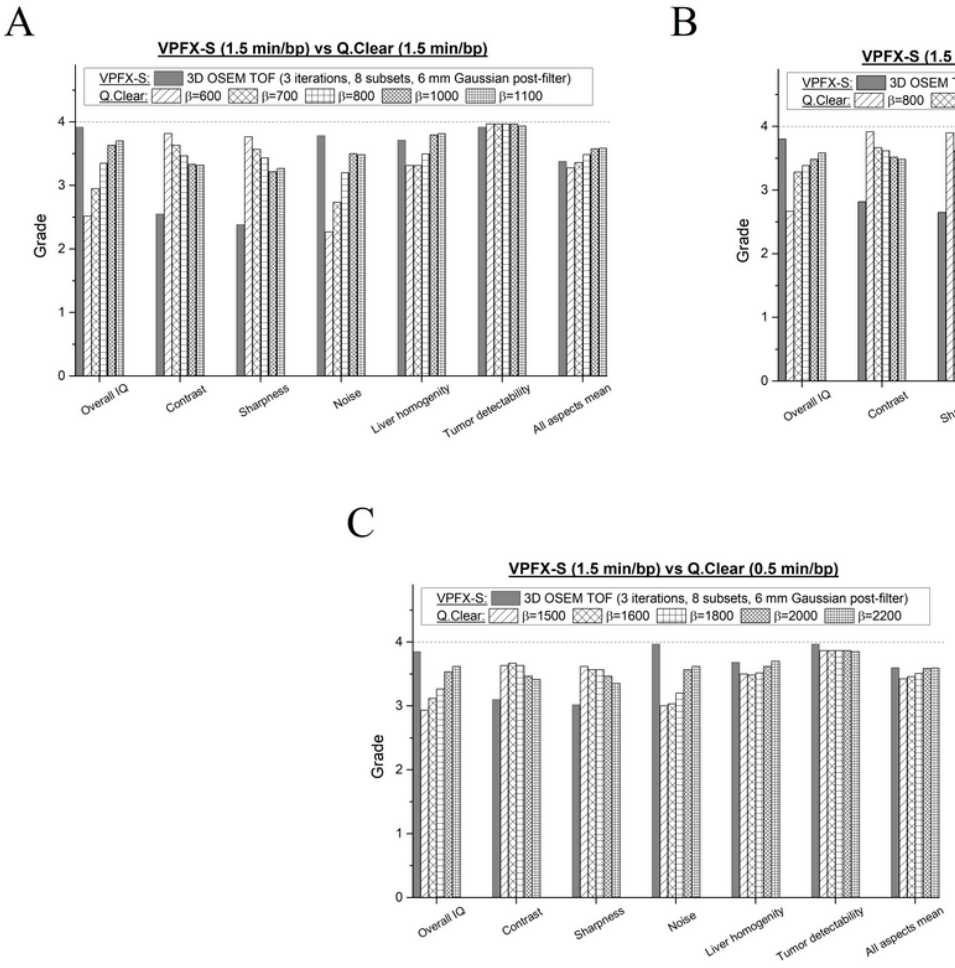

Figure 7

Mean of visual assessment (overall image quality, contrast, sharpness, noise level, liver homogeneity, tumor detectability and mean of all rated aspects) done by two experienced nuclear medicine physicians for Q.Clear reconstructions with different β values and (A) 1.5 min/bp, (B) 1.0 min/bp and (C) 0.5 min/bp and for the gold standard recontruction (VPFX-S, 1.5 min/bp) following a 4-point scale (1, very poor/nondiagnostic; 2, poor; 3, good and 4, very good).

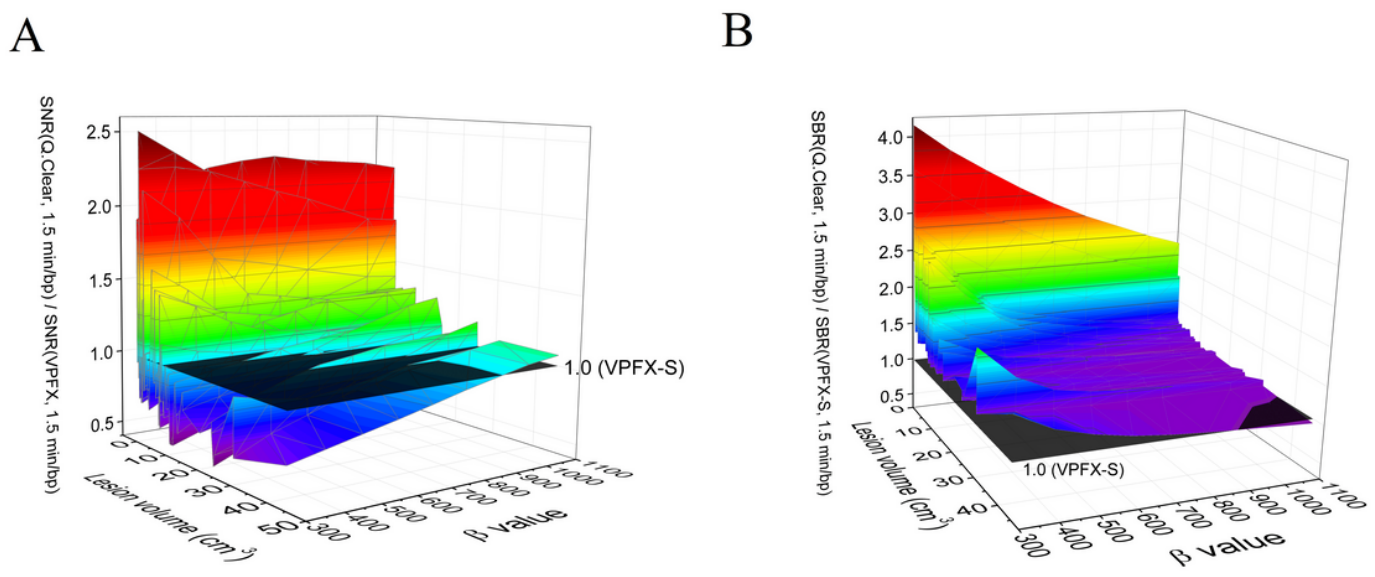

Figure 8

Improvement of (A) SNR and (B) SBR using Q.Clear with 1.5 min/bp as a function of the β penalization factor and tumor lesions volume compared to VPFX-S. 1.5 min/bp.